p53-inducible DPYSL4 associates with mitochondrial supercomplexes and regulates energy metabolism in adipocytes and cancer cells

Hidekazu Nagano[a,b], Naoko Hashimoto[b,c], Akitoshi Nakayama[b,c], Sawako Suzuki[a,b], Yui Miyabayashi[c], Azusa Yamato[b,c], Seiichiro Higuchi[b,c], Masanori Fujimoto[a,b], Ikki Sakuma[a,b], Minako Beppu[b,c], Masataka Yokoyama[b,c], Yutaka Suzuki[d], Sumio Sugano[d], Kazuhiro Ikeda[e], Ichiro Tatsuno[f], Ichiro Manabe[g], Koutaro Yokote[a], Satoshi Inoue[e,h], and Tomoaki Tanaka[b,c,1]

[a]Department of Clinical Cell Biology and Medicine, Graduate School of Medicine, Chiba University, 260-8670 Chiba, Japan; [b]Japan Agency for Medical Research and Development-Core Research for Evolutional Science and Technology, 100-8055 Tokyo, Japan; [c]Department of Molecular Diagnosis, Graduate School of Medicine, Chiba University, 260-8670 Chiba, Japan; [d]Department of Medical Genome Sciences, Graduate School of Frontier Sciences, University of Tokyo, 277-8562 Chiba, Japan; [e]Division of Gene Regulation and Signal Transduction, Research Center for Genomic Medicine, Saitama Medical University, 350-1241 Saitama, Japan; [f]Center for Diabetes, Metabolism and Endocrinology, Toho University Sakura Medical Center, 285-8741 Chiba, Japan; [g]Department of Disease Biology and Molecular Medicine, Graduate School of Medicine, Chiba University, 260-8670 Chiba, Japan; and [h]Department of Functional Biogerontology, Tokyo Metropolitan Institute of Gerontology, 173-0015 Tokyo, Japan

The tumor suppressor p53 regulates multiple cellular functions, including energy metabolism. Metabolic deregulation is implicated in the pathogenesis of some cancers and in metabolic disorders and may result from the inactivation of p53 functions. Using RNA sequencing and ChIP sequencing of cancer cells and preadipocytes, we demonstrate that p53 modulates several metabolic processes via the transactivation of energy metabolism genes including dihydropyrimidinase-like 4 (*DPYSL4*). *DPYSL4* is a member of the collapsin response mediator protein family, which is involved in cancer invasion and progression. Intriguingly, DPYSL4 overexpression in cancer cells and preadipocytes up-regulated ATP production and oxygen consumption, while DPYSL4 knockdown using siRNA or CRISPR/Cas9 down-regulated energy production. Furthermore, DPYSL4 was associated with mitochondrial supercomplexes, and deletion of its dihydropyrimidinase-like domain abolished its association and its ability to stimulate ATP production and suppress the cancer cell invasion. Mouse-xenograft and lung-metastasis models indicated that DPYSL4 expression compromised tumor growth and metastasis in vivo. Consistently, database analyses demonstrated that low *DPYSL4* expression was significantly associated with poor survival of breast and ovarian cancers in accordance with its reduced expression in certain types of cancer tissues. Moreover, immunohistochemical analysis using the adipose tissue of obese patients revealed that DPYSL4 expression was positively correlated with *INFg* and body mass index in accordance with p53 activation. Together, these results suggest that DPYSL4 plays a key role in the tumor-suppressor function of p53 by regulating oxidative phosphorylation and the cellular energy supply via its association with mitochondrial supercomplexes, possibly linking to the pathophysiology of both cancer and obesity.

tumor suppressor p53 | mitochondria | metabolism | cancer | obesity

The altered metabolism of cancer cells plays a pivotal role in the pathogenesis and progression of a variety of cancers. Similarly, the regulation of intracellular metabolic processes has a profound effect on the development of many metabolic disorders, such as diabetes mellitus and obesity. Changes in metabolic processes, including glucose uptake and glycolysis, lactate production, glutaminolysis, and lipid biosynthesis, may be either a cause or a consequence of tumorigenesis or metabolic disease (1, 2). In this context, several recent lines of evidence implicate p53 in the regulation of cellular metabolism, energy production, autophagy, and reactive oxygen species (ROS) levels (3–5). In fact, p53 suppresses glycolysis by down-regulating the expression of glucose transporters both directly and indirectly through NF-κB signaling

(6) and by up-regulating the expression of TP53-induced glycolysis regulatory phosphatase, which reduces fructose-2,6-bisphosphate levels (7). Conversely, p53-responsive elements are present in the promoters of phosphoglycerate mutase, which catalyzes one of the late steps in glycolysis (8), and p53 also transactivates hexokinase II, a key enzyme in a glycolytic pathway.

In addition to its antagonistic effects on at least some steps of the glycolytic pathway (5), p53 controls glutamine metabolism through the mitochondrial phosphate-activated glutaminase GLS2, which regulates glutathione synthesis and energy production via α-ketoglutarate. These activities are postulated to contribute to the tumor suppressor function of GLS2 as a p53-target gene (9, 10). Accordingly, p53 has been shown to help maintain mitochondrial function (11, 12) and to drive oxidative phosphorylation (OXPHOS) via the activation of subunit I of cytochrome *c* oxidase (SCO2) transcription (13, 14) and the induction of the ribonucleotide reductase subunit p53R2 (15). Thus, as the recent evidence linking p53 to the regulation of energy metabolism and multifaceted mitochondrial

Significance

We herein performed RNA sequencing to show that DPYSL4 is a p53-inducible regulator of energy metabolism in both cancer cells and normal cells, such as adipocytes. DPYSL4 was found to localize in both cytosol and mitochondria, particularly in associations with mitochondrial supercomplexes, providing a potential mechanism for its regulation of OXPHOS and cellular energy supply. Furthermore, DPYSL4 expression suppressed tumor growth and metastasis in vivo. Together, these results suggest a potential link between p53-inducible DPYSL4 and the pathophysiology of cancer and metabolic disorders, possibly via its energy-regulating function.

functions has been shown, it suggests that p53 plays roles in both the regulation of cancer metabolism and the reactions of cells and tissues to metabolic or other oxidative stresses.

Mitochondrial OXPHOS and cytoplasmic glycolysis function coordinately to support mitochondrial processes such as ATP generation. During mitochondrial OXPHOS, oxygen is reduced to water by cytochrome *c* oxidase in the final stage of the electron transport chain via four mitochondrial protein complexes—NADH-Q oxidoreductase, succinate-Q reductase, Q-cytochrome *c* oxidoreductase, and cytochrome *c* oxidase (also known as complexes I, II, III, and IV, respectively), and one complex for ATP synthesis (complex V or F1-F10 ATPase). Several lines of evidence suggest that complex V forms dimeric (16) and oligomeric structures (1, 17) with complexes I, III, and IV in the mitochondrial membrane, resulting in stoichiometric supercomplexes known as respirasomes (18) and even larger structures known as respiratory strings (19). OXPHOS dysfunction caused by defects in the activity or formation of those supercomplexes is tightly linked to the pathogenesis of a variety of human diseases, including cancer, aging, degenerative disorders, diabetes, and metabolic syndrome.

In this study, we used RNA sequencing to show that DPYSL4 is a p53-inducible regulator of energy metabolism in both cancer cells and normal cells, such as adipocytes. Furthermore, DPYSL4 localized partly in the mitochondria, where it was able to associate with mitochondrial supercomplexes, providing a potential mechanism for the regulation of OXPHOS and cellular energy supply. Together, these results suggest a potential link between DPYSL4 and the pathogenesis of cancer and metabolic disorders.

Results

DPYSL4 Is a Common p53 Target in Cancer Cells and Adipocytes.

Cancer cells acquire certain important characteristics, including a unique metabolic phenotype, upon transformation and metastasis. Some of these characteristics are also associated with the regulation of preadipocyte function, as well as the differentiation of adipocytes, pointing to commonalities between the mechanisms of pathogenesis associated with oncogenesis and adipogenesis (20). To investigate the commonalities in p53-dependent metabolic regulation between adipocytes and cancer cells, we performed RNA-seq analysis with two distinct systems: (*i*) H1299 cells infected with adenoviruses expressing either p53 or LacZ and (*ii*) preadipocytes treated with doxorubicin to induce DNA damage or untreated. We identified 555 differentially expressed genes (DEGs) in the H1299 cells; of these, 502 genes were up-regulated in the cells expressing p53 compared with those expressing LacZ, and 53 genes were down-regulated in the cells expressing p53. We also identified 284 DEGs in the preadipocytes with 228 genes up-regulated in the cells with treatment-induced DNA damage and 56 genes down-regulated in the cells with treatment-induced DNA damage compared with untreated cells (Fig. 1*A* and *SI Appendix*, Fig. S1 *A–C*). Accordingly, 60 DEGs appeared in both cell types as common potential p53 targets (*SI Appendix*, Table S1), including some previously reported p53 targets proline dehydrogenase 1 (*PRODH*) and glutaminase 2 (*GLS2*), but lacked other classical p53 targets, such as *CDKN1A* and *PIG3*. The level of *DPYSL4* (Gene ID 10570) was drastically induced, by 7.70-fold log$_2$ (intensity), in H1299 cells expressing p53, and by 6.07-fold log$_2$ (intensity) in preadipocytes with DNA damage, suggesting that this gene is important to p53 function in both cancer cells and adipocytes (Fig. 1*B*). Consistent with these observations, transcriptional start site (TSS) and RNA-seq analyses confirmed transcription and induction of selected genes, including DPYSL4, in both H1299 cells and adipocytes. The human *DPYSL4* gene contains 14 coding exons and is located on chromosome 10q26. Chromatin immunoprecipitation (ChIP)-sequence analysis showed that p53 bound to multiple sites within the *DPYSL4* genetic locus (introns 1, 2, 3, and 4) and that the induction of *DPYSL4* transcription was associated with AcH3 and 3MeK4H3 (Fig. 1 *C* and *D*).

To examine the p53-dependent induction of DPYSL4 at the protein level, we cloned the human DPYSL4 gene and generated anti-DPYSL4 antibodies. Anti-FLAG M2 antibodies and anti-DPYSL4 antibodies, corresponding to the 500/514 and 545/561 epitopes, respectively, both recognized DPYSL4-FLAG as an 65-kDa band (*SI Appendix*, Fig. S2*A*) and were capable of detecting endogenous DPYSL4 (*SI Appendix*, Fig. S2*B*; see asterisk). Genotoxic stress with doxorubicin or daunorubicin treatment induced DPYSL4 at both the protein and mRNA levels in p53-dependent manner in HCT116, A549, MCF-7 cells, and preadicpocytes (Fig. 1 *E–J* and *SI Appendix*, S2 *C* and *D*). Furthermore, the silencing of
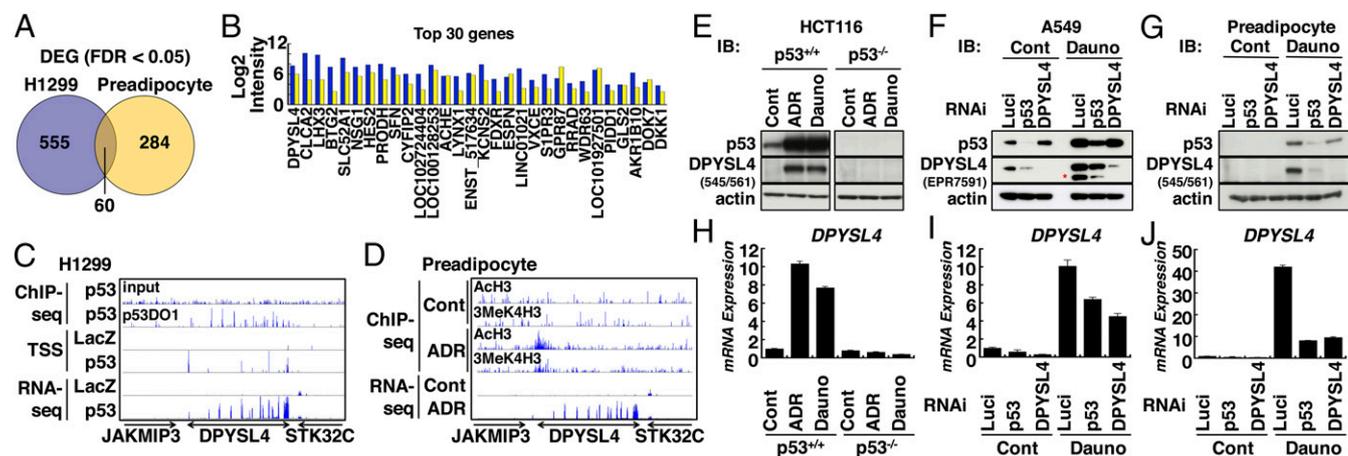

Fig. 1. Identification of DPYSL4 as a p53-inducible gene in H1299 cells and preadipocytes. (*A*) Common p53-inducible genes in H1299 cells and preadipocytes determined by RNA-seq. H1299 cells were infected with adenoviruses expressing either LacZ or p53 for 24 h. Human preadipocytes were either untreated (Cont) or treated with doxorubicin (ADR; 1 μM) for 24 h. A Venn diagram shows the DEGs in H1299 cells (left circle in blue) and preadipocytes after DNA damage (right circle in yellow). FDR, false discovery rate. (*B*) The bar graph shows the top DEGs in H1299 cells (blue bar) and preadipocytes (yellow bar). (*C*) p53-ChIP, TSS, and RNA-seq of the *DPYSL4* loci in H1299 cells. H1299 cells were infected with adenoviruses expressing either LacZ or p53 for 24 h. (*D*) ChIP-seq for AcH3 and 3meK4H3 and RNA-seq at *DPYSL4* loci in human preadipocytes upon DNA damage. Human preadipocytes were either untreated (Cont) or treated with doxorubicin (1 μM) for 24 h. (*E* and *H*) HCT116 p53$^{+/+}$ or p53$^{-/-}$ cells were treated with doxorubicin (ADR; 1 μM) or daunorubicin (Dauno; 1 μM) followed by immunoblotting to detect p53, DPYSL4, and actin and real-time RT-PCR analysis of *DPYSL4* expression normalized by *L32 mRNA*. A549 cells (*F* and *I*) and preadipocytes (*G* and *J*) were transfected with luciferase RNAi (Luci), p53 RNAi, or DPYSL4 RNAi for 24 h. Then, the cells were either untreated (Cont) or treated with Dauno (1 μM and 0.5 μM for A549 and preadipocytes, respectively) for another 24 h. Immunoblotting to detect p53, DPYSL4, and actin and real-time RT-PCR analysis to determine the expression levels of *DPYSL4* mRNA were performed. Asterisk shows that the minor band was detected with an anti-DPYSL4 antibody (EPR7591).

p53 or DPYSL4 with siRNA significantly inhibited the induction of DPYSL4 (Fig. 1 *F*, *G*, *I*, and *J*).

Our results indicated that DPYSL4 was up-regulated as a p53 target in both preadipocytes and tumor cells, although the extent of its induction varied by cell type and/or the level and nature of the stress imposed on the cells. Notably, p53 did not induce the mRNA expression of other DPYSL family members in H1299 cells or in preadipocytes (*SI Appendix*, Fig. S3 *A* and *B*).

DPYSL4 Associates with Mitochondrial Supercomplexes. To address the function of DPYSL4, we first examined its subcellular localization using confocal microscopy. Following induction in response to cellular stress, endogenous DPYSL4 accumulated in the cytoplasm and partially in the mitochondria, as evidenced by costaining with Mitotracker (Fig. 2*A*, *Upper*) or NDUFA9, a component of mitochondrial complex I (Fig. 2*A*, *Lower*) in HS68 cells and preadipocytes, respectively. To confirm the presence of DPYSL4 in mitochondria, we fractionated the cytoplasm and mitochondria and then performed immunoblotting with anti-FLAG or anti-DPYSL4 and antibodies against components of the OXPHOS mitochondrial membrane–protein complexes I–V. We detected both ectopically expressed FLAG-DPYSL4 (Fig. 2*B*) and endogenous DPYSL4 (Fig. 2*C*) not only in the cytoplasm but also in the mitochondria as confirmed by a knockout of DPYSL4 using the CRISPR-Cas9 system (Fig. 2*C*). Concomitantly, the components of the mitochondrial complexes were detected only in the mitochondrial fraction (Fig. 2 *B* and *C*).

As mentioned above, the mitochondrial complexes are not randomly distributed within the inner mitochondrial membrane but are instead assembled into supramolecular structures. Because the proposed functional roles of respiratory supercomplexes include catalytic enhancement, substrate channeling, the sequestration of reactive intermediates, and the stabilization of individual complexes within the supercomplexes, and because the distribution patterns of complexes I–V vary with growth conditions and cell types (21), we sought to determine whether DPYSL4 was associated with specific mitochondrial supercomplexes. We infected H1299 cells with DPYSL4-FLAG or Mock lentivirus and then fractionated the mitochondria. We solubilized the mitochondria with dodecylmaltoside (DDM) and then subjected them to 2D Blue Native SDS polyacrylamide gel electrophoresis (BN/SDS/PAGE) followed by immunoblotting with various antibodies, as described in *SI Appendix, Supplementary Materials and Methods* (Fig. 2 *D–F*). Consistent with previous results, we observed a supercomplex comprising complexes I, III, and IV in H1299 cells (Fig. 2 *D* and *E*) (22, 23). We detected DPYSL4 in the exact position on the gels as that occupied by NADH:ubiquinone oxidoreductase core subunit V1 (NDUFV1), a component of complex I, as well as by Rieske iron-sulfur polypeptide 1 (RISP) and cytochrome C oxidase (COX) subunit 4, components of complexes III and IV, respectively. In addition, endogenous DPYSL4 was detected in association with the mitochondrial supercomplexes in preadipocytes similarly (Fig. 2*F*). Given that, in mammalian mitochondria, almost all of complex I is assembled into supercomplexes containing complexes $I/III_2/IV_n$, we propose that DPYSL4 associates with these mitochondrial supercomplexes to affect energy regulation through OXPHOS.

DPYSL4 Modulates Intracellular ATP Production and Oxygen Consumption by Up-Regulating Mitochondrial Respiration. Our results thus far suggest that DPYSL4 is a p53-inducible regulator of mitochondrial function. Therefore, we sought to determine whether DPYSL4 directly affects OXPHOS and ATP production in the mitochondria. Metabolome analysis permits characterization and validation of the metabolic states of various cells and tissues and is useful for documenting direct information about energy metabolism as well as the relationships between metabolic networks and underlying gene effects. We performed a capillary electrophoresis time-of-flight mass spectrometry-based metabolomics analysis using HCT116 cells with or without p53 expression. As expected based on the notion that most cancer cells predominantly produce energy by glycolysis rather than by OXPHOS, we detected high concentrations of glycolytic
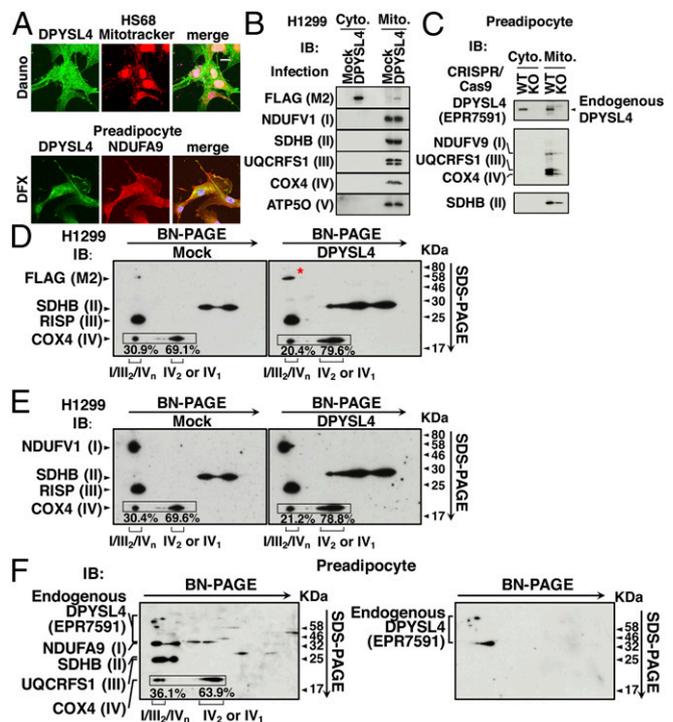

Fig. 2. DPYSL4 partially localizes to mitochondria and associates with mitochondrial supercomplexes. (*A*) HDF cells and preadipocytes were treated with daunorubicin (Dauno, 1 μM) for 24 h and with desferrioxamine (DFX, 300 μM) for 12 h, respectively, and then subjected to confocal microscopic analyses using an anti-DPYSL4 antibody along with Mitotracker (*Upper*) or an anti-NDUFA9 antibody (*Lower*). Nuclei were counterstained with DAPI. (*B*) H1299 cells were either mock-infected or infected with lentivirus expressing DPYSL4 for 3 d and then subjected to mitochondrial fractionation. Immunoblotting was performed to detect DPYSL4-FLAG and the indicated components of mitochondrial complex proteins in the cytosolic and mitochondrial fractions. (*C*) DPYSL4 was either not (WT) or knocked out (KO) using the CRISPR/Cas9 system in preadipocytes. Immunoblotting performed to detect endogenous DPYSL4 indicated components of mitochondrial supercomplexes in the cytosolic and mitochondrial fractions. (*D* and *E*) Identification of mitochondrial supercomplexes and their association with DPYSL4 in H1299 cells. Cells were treated as in *B* for 3 d and then subjected to mitochondrial supercomplex assay and analysis by 2D resolution of BN-PAGE followed by SDS/PAGE. Immunoblotting was performed with anti-FLAG M2 to detect DPYSL4-FLAG (red asterisk). and with anti-NDUFV1, anti-SDHB, anti-RISP, and anti-COX4 to detect complexes I, II, III, and IV, respectively. (*F*) The identification of mitochondrial supercomplexes and their association with endogenous DPYSL4 in preadipocytes. Immunoblotting was performed with only anti-DPYSL4 (*Right*) or along with anti-NDUFA9, anti-SDHB, anti-UQCRFS1, and anti-COX4 to detect complexes I, II, III, and IV, respectively (*Left*).

intermediates glucose-6-phosphate (G6P), fructose-6-phosphate (F6P), and fructose-1,6-bisphosphate (F1,6BP), in accordance with the up-regulation of lactate in $p53^{-/-}$ cells, indicating that p53 has a countering effect on the enhanced glycolysis in cancer cells (*SI Appendix*, Fig. S4*A*).

To probe the precise role of DPYSL4 in the effects of p53 on metabolic regulation, we next examined the effects of siRNA silencing of p53 or DPYSL4 on the metabolomic profile of HCT116 $p53^{+/+}$ cells (*SI Appendix*, Fig. S4*B*). The difference in metabolic profiles between cells transfected with siRNAs targeting luciferase and p53, respectively, was similar to that between HCT116 $p53^{-/-}$ cells and HCT116 $p53^{+/+}$ cells, although the difference induced by RNAi was smaller and not significant. In contrast, DPYSL4 silencing by siRNA showed similar trends toward the elevation of oncometabolites (succinate, fumarate, and malate) but not for the glycolytic metabolites F1,6BP and NAD^+, compared with p53 silencing by siRNA (*SI Appendix*, Fig. S4 *A* and *B*), indicating that

DPYSL4 may directly influence the regulation of the TCA cycle rather than that of the upstream steps of the glycolytic pathway, in accordance with its association with mitochondrial supercomplexes.

To further investigate the functional role of DPYSL4 in mitochondrial respiration, we examined the oxygen consumption rate (OCR) using a flux analyzer. The OCR of HCT116 $p53^{+/+}$ cells was higher than that of HCT116 $p53^{-/-}$ cells. Both p53 silencing and DPYSL4 silencing resulted in a lower OCR than did treatment with a control siRNA (Fig. 3A). Both DPYSL4 silencing and p53 silencing in HCT116 $p53^{+/+}$ cells significantly suppressed basal respiration, maximal respiration, and ATP production to the same levels as those observed in HCT116 $p53^{-/-}$ cells (Fig. 3B). Likewise, the silencing of p53 or DPYSL4 by siRNA in HCT116 $p53^{+/+}$ cells increased the NAD^+/NADH ratio to the same level observed in HCT116 $p53^{-/-}$ cells (Fig. 3C), supporting a direct role for DPYSL4 in mitochondrial respiration.

DPYSL4 Functions as a Tumor Suppressor by Regulating Energy Metabolism. Next, we investigated the physiological effects of DPYSL4 on cellular proliferation in vitro and in vivo. The overexpression of p53 or DPYSL4-FLAG in H1299 cells led to a significant reduction in Matrigel invasion (Fig. 3D). That effect was reversed in a DPYSL4 deletion mutant (Δmid), which harbored a deletion of amino acids 194–243, a region similar to the active site of the dihydropyrimidinase (DHP) domain in the DHP enzyme (Fig. 3 D and E). Consistent with this finding, the overexpression of full-length DPYSL4 (FL-DPYSL4) led to an elevated OCR, whereas overexpression of Δmid did not, in both H1299 cells and pre-adipocytes (Fig. 3F and SI Appendix, Fig. S5A). Additionally, basal respiration, maximal respiration, and ATP production were significantly up-regulated in the presence of FL-DPYSL4, but not Δmid (Fig. 3G and SI Appendix, Fig. S5A). In line with its loss of function in energy regulation, Δmid abolished its interaction with supercomplexes comprising complexes I, III, and IV in H1299 cells, as revealed by 2D BN/SDS/PAGE analysis (Fig. 3H). Thus, these results indicated that DPYSL4 plays a positive role in energy

production, possibly through OXPHOS modulation via association with the mitochondrial supercomplexes.

To further document the functional role of endogenous DPYSL4 in positively regulating mitochondrial respiration in the p53 pathway, we performed flux analysis in combination with the CRISPR/Cas9 system in preadipocytes. As expected, a knockout of p53 or DPYSL4 by the CRISPR/Cas9 system showed a similar trend toward reduction in basal respiration, maximal respiration, and ATP production in preadipocytes (Fig. 3 I–K) as in HCT116 cells (Fig. 3A). Furthermore, restoration of FL-DPYSL4, but not Δmid, recovered the inhibitory effect of p53 knockout and DPYSL4 knockdown on mitochondrial respiration in preadipocytes (SI Appendix, Fig. S5 B and C).

Next, to assess the tumor-suppressor function of DPYSL4 in vivo, we examined mouse xenograft and lung metastasis models using H1299 cells with or without DPYSL4 expression (Fig. 4 A and B). Consistent with our findings, DPYSL4 expression significantly reduced tumor growth and lung metastasis in vivo. Furthermore, analysis of the expression profiles of matched tumor and normal tissues in the Oncomine database (24) and The Cancer Genome Atlas (TCGA) database (https://cancergenome.nih.gov/) revealed that the expression of DPYSL4 mRNA was decreased in cancer tissues, such as cervix squamous cell carcinoma, invasive ductal breast carcinoma, and pancreatic carcinoma (Fig. 4C). Importantly, a Kaplan–Meier survival analysis using the KM-plotter database (25, 26) demonstrated that low expression of *DPYSL4* correlated significantly with poor survival outcome in patients with breast and ovarian cancers (Fig. 4D). Taken together, our results suggest that DPYSL4 plays a role in tumor suppression, at least in certain types of cancers.

p53 Activation and DPYSL4 Up-Regulation with Inflammation in the Adipose Tissue of Obese Patients. To address the physiological role of DPYSL4 in adipocytes, we examined the expression profile and clinical relationships of this protein using visceral fat tissues (perirenal fat tissues) from 18 nonobese patients and 22 obese patients. Consistently, the mean body mass index (BMI) of the
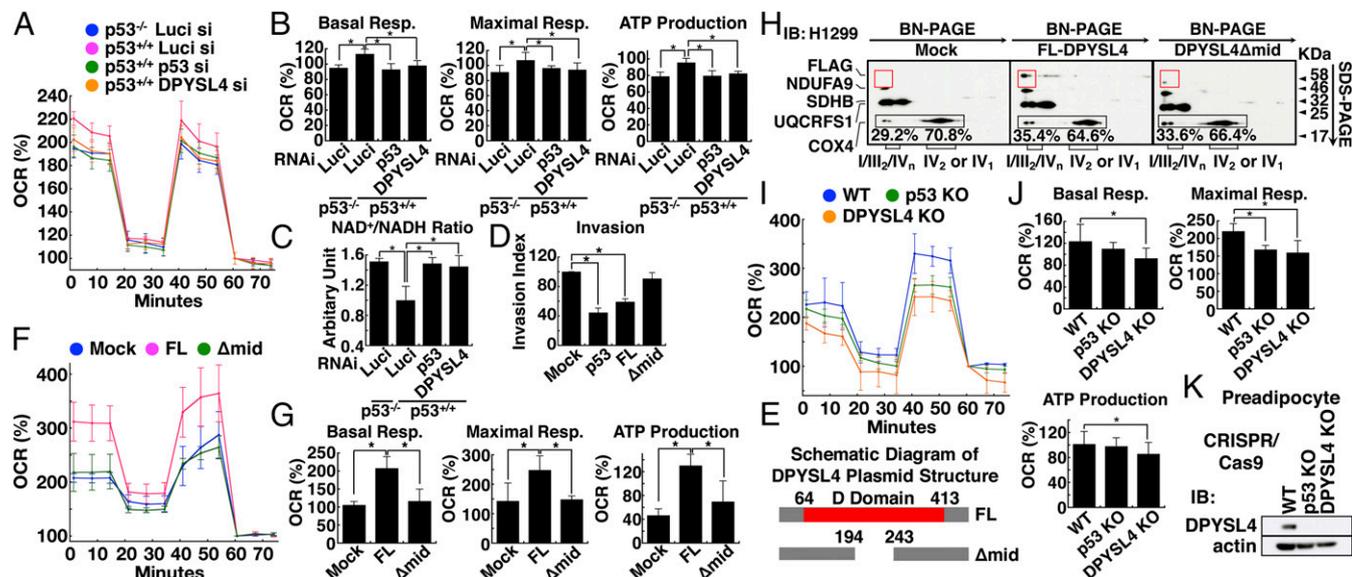

Fig. 3. DPYSL4 is a potential regulator of ATP production and oxidative phosphorylation, and the D domain of DPYSL4 is important for ATP production and tumor-cell invasion. (A and B) After HCT116 $p53^{+/+}$ cells were treated with Luci, p53, or DPYSL4 RNAi for 48 h, the OCR was recorded by flux analyzer. The OCR was measured at baseline and after treatment with oligomycin, FCCP, and mixture of antimycin and rotenone. (C) Similarly, the NAD^+/NADH ratio was measured (*$P < 0.05$). (D) The graph shows the average invasion index of three independent experiments with error bars representing the SD. (E) A schematic representation of cDNA constructs of the full-length DPYSL4 (FL) and DPYSL4 lacking amino acids 194–243 (Δmid). (F and G) After H1299 cells overexpressed mock, FL-DPYSL4 (FL), or DPYSL4Δmid (Δmid) for 72 h, the OCR was recorded by flux analyzer (*$P < 0.05$). (H) The identification of mitochondrial super-complexes and their association with FL, but not Δmid, in H1299 cells. (I and J) In preadipocytes of WT or p53 KO and DPYSL4 KO using CRISPR/Cas9, the OCR was recorded by flux analyzer (*$P < 0.05$). (K) Immunoblotting was performed to evaluate the knockout efficacy of endogenous DPYSL4.
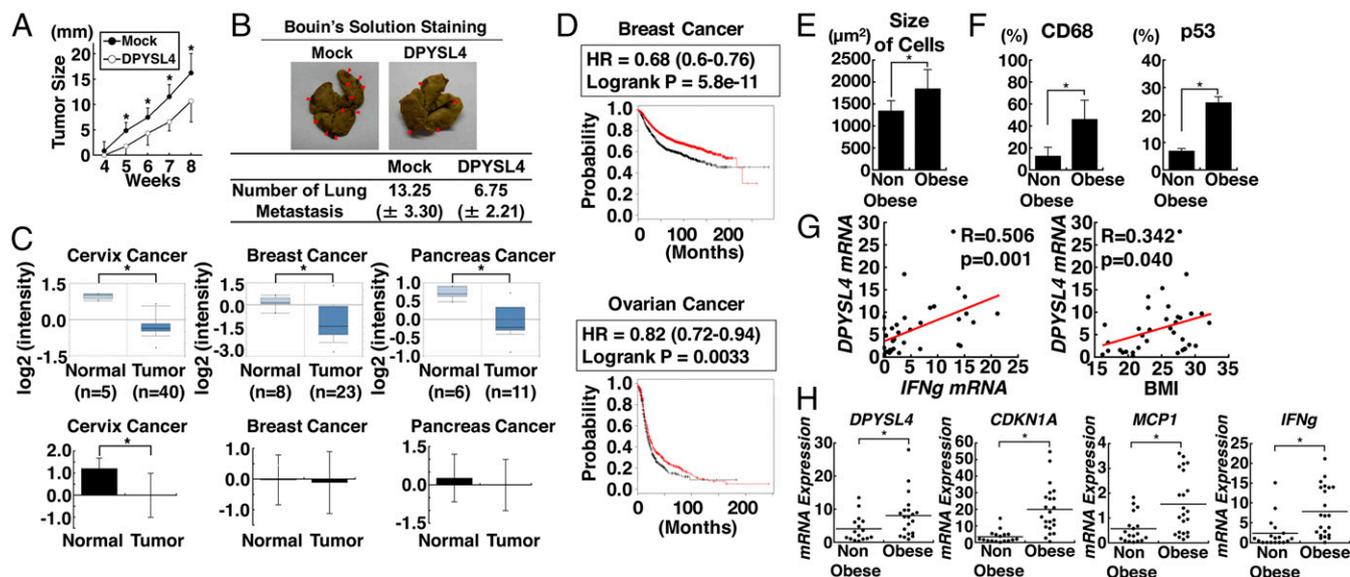
CELL BIOLOGY

Fig. 4. Loss of DPYSL4 expression in various cancer tissues and the potential tumor suppressor function of DPYSL4 in vivo and p53 activation and DPYSL4 up-regulation in human adipose tissue from obese patients. (*A* and *B*) H1299 cells were mock-infected or infected with lentivirus expressing DPYSL4 for 3 d, and then injected into a xenograft model or a lung-metastasis model with NOD/SCID mice. Tumor growth was measured over time. The red arrows show metastasis. (*C*) The loss or reduction of *DPYSL4* mRNA expression in indicated human cancer tissues based on analysis using the Oncomine database and TCGA (*$P < 0.05$). (*D*) Kaplan–Meier analyses were performed using the KM-plotter database (kmplot.com/analysis/). Graphs represent survival curve in comparison between DPYSL4 high (red) and DPYSL4 low (black) in breast and ovarian cancer. (*E*) The sizes of adipocytes in nonobese and obese patients are shown. (*F*) Immunohistology of human adipose tissue. p53- or CD68-positive cells and -negative cells were counted, and positive rates were calculated. (*G*) Correlations between the mRNA expression of *DPYSL4* and that of IFN-γ and BMI (*$P < 0.05$). (*H*) mRNA expression of *DPYSL4*, *CDKNA1*, *MCP1*, and *IFNg* was normalized by L32 expression and then analyzed in adipose tissues.

nonobese and obese patients was 20.1 (16.1–23.2) kg/m^2 and 28.1 (25.1–32.1) kg/m^2, respectively. The adipocytes of the obese patients were significantly enlarged compared with those of the nonobese patients (Fig. 4*E*). Immunohistology of adipose tissues demonstrated that p53 was significantly up-regulated concomitant with marked infiltration of CD68-positive cells in adipose tissues of obese patients (Fig. 4*F* and *SI Appendix*, Fig. S6). In agreement with our in vitro results, the mRNA levels of *DPYSL4*, *CDKN1A*, *MCP1*, and *IFNg* were higher in the adipose tissues of the obese patients compared with those in the nonobese patients (Fig. 4*H*). Accordingly, Pearson correlation analysis revealed that *DPYSL4* expression was positively correlated with both IFN-γ (*IFNg*) levels and BMI (Fig. 4*G*). Taken together, these results indicate a pathophysiological relationship between p53 activation and inflammatory cytokines, leading to the up-regulation of DPYSL4 in human adipose tissue of obese patients.

Discussion

The DPYSL family is also known as the collapsin response mediator protein (CRMP) family, which includes five cytosolic proteins that share 50–75% amino acid sequence homology and can form heterotetramers (27). Originally identified as mediators of semaphorin 3A signaling, CRMPs are highly expressed in the nervous system, where they function to inhibit extension of the axonal growth cone during neuronal development (28, 29). Various malignant tumors display altered CRMP expression. For instance, CRMP1/DPYSL1 was identified as a potential invasion-suppressor gene in highly progressive lung cancer cells (30). Conversely, a long isoform of CRMP1 was recently identified as an enhancer of cancer invasion (31). High levels of nuclear-phosphorylated CRMP2/DPYSL2 correlated with poor prognosis in nonsmall cell lung carcinoma, whereas CRMP5/DPYSL5 is highly expressed in high-grade neuroendocrine lung tumors but not in low-grade neuroendocrine lung tumors or squamous cell carcinomas (32).

The expression and pathological functions of CRMP3/DPYSL4 in cancer tissues are not well understood. Our results indicate that

DPYSL4 has a tumor suppressor function associated with mitochondrial supercomplexes and energy regulation through OXPHOS. Cancer cells have altered metabolism to support the increased nutrient consumption that is required for their high rate of proliferation (21). Supercomplex assembly is dynamic and organizes electron flux to optimize the use of available substrates (33). For instance, COX subunit 7a-related polypeptide (COX7RP, also known as COX7A2L or SCAF1) is required for the interaction between complexes III and IV. Specific regions in COX7RP interact with complexes III and IV, and this interaction requires the correct orientation of a histidine residue at position 73 (34). COX7RP is thought to be a key molecule that promotes supercomplex assembly, especially the supercomplex of complexes III$_2$/IV$_n$ with complex I (23, 35). Given that the formation and/or deterioration of the supercomplex is tissue-specific and variable in pathophysiological conditions (33–36), to more thoroughly describe supercomplex formation factors, influences, such as environment, nutrition factors, signals, and metabolic regulation, associated with supercomplex formation must be examined. Here, we detected DPYSL4 in association with complexes I, III, and IV factors (Fig. 2 *D–F*), suggesting that DPYSL4 associates with supercomplex assembly to influence energy regulation through OXPHOS.

Most cells exhibit high ATP/ADP and NADH/NAD$^+$ ratios during proliferation. To produce energy for growth, cells first convert glucose into acetyl-CoA in the mitochondrial matrix. The acetyl-CoA subsequently feeds into the TCA cycle and various synthetic pathways to produce fatty acids, nucleic acids, and amino acids (1). Therefore, it is not surprising that proliferating cancer cells rely heavily on aerobic glycolysis for energy production, a phenomenon known as the Warburg effect. The p53 protein has multiple roles in the regulation of intracellular metabolic pathways, including glycolysis, glutaminolysis, lipid metabolism, and glutathione synthesis, and each of these roles may contribute to its tumor suppressor function (7, 37). We observed that the levels of TCA intermediates and lactate production in HCT116 p53$^{+/+}$ cells with siRNA-induced silencing of p53 or DPYSL4 were similar to those in HCT116 p53$^{-/-}$ cells, whereas the levels of glycolytic

intermediates were unaffected by silencing of these same genes (*SI Appendix*, Fig. S4B). Paraganglioma, kidney cancer, and breast cancer have each been shown to harbor mutations in genes encoding metabolic enzymes, such as succinate dehydrogenase, fumarate hydratase, and isocitrate dehydrogenase (21, 38). Our results demonstrate that DPYSL4 may counteract the action of the Warburg effect via its association with mitochondrial supercomplexes to support OXPHOS. Besides, given that DPYSL4 is present in both cytoplasm and mitochondria, there might be potential additional mechanisms that contribute to the tumor suppressive function of DPYSL4.

With respect to adipogenesis, we demonstrated that DPYSL4 and p53 are expressed in adipocytes and adipose tissues. The expression of p53 in adipose tissue is associated with metabolic disorders and plays a functional role in the development of insulin resistance (39), which induces hyperinsulinemia and tumorigenesis; however, little is known about how p53 or which p53-inducible genes affect pathophysiology of adipose tissue. Intriguingly, our RNA-seq analysis of cancer cells and preadipocytes identified several mitochondria-related genes with p53-dependent expression. For instance, BTG2 was previously reported to be a putative tumor suppressor and ROS regulator in mitochondria (40, 41), and SLC8A3, also known as NCX3, was previously shown to localize in mitochondria and improve neuron survival through the extrusion of Ca^{2+} (42). The similarities in the expression of p53 and p53-inducible genes such as DPYSL4 in adipocytes and cancer cells suggest that p53 and some of its direct targets are involved in the pathogenesis of both cancer and obesity.

In conclusion, our results demonstrate that p53-induced DPYSL4 has a tumor suppressor function associated with OXPHOS regulation. DPYSL4 improves intracellular energy metabolism by localizing with mitochondrial supercomplexes and regulating steps of the TCA cycle and, thereby, may have functional consequences in both cancer and adipose tissue.

Methods

H1299 human nonsmall cell lung cancer cells, A549 human alveolar epithelial cells, MCF-7 human breast cancer cells, HCT116 human colon cancer cells, and human dermal fibroblasts (HDFs) were cultured in DMEM with 10% FBS and antibiotics. We cultured human preadipocytes derived from human abdominal visceral fat in MesenPRO RSTM Medium (Gibco) with antibiotics.

Details for the other methods can be found in *SI Appendix, Supplementary Materials and Methods*.

1. Vander Heiden MG, Cantley LC, Thompson CB (2009) Understanding the Warburg effect: The metabolic requirements of cell proliferation. *Science* 324:1029–1033.
2. Berkers CR, Maddocks OD, Cheung EC, Mor I, Vousden KH (2013) Metabolic regulation by p53 family members. *Cell Metab* 18:617–633.
3. Deberardinis RJ, Sayed N, Ditsworth D, Thompson CB (2008) Brick by brick: Metabolism and tumor cell growth. *Curr Opin Genet Dev* 18:54–61.
4. Kroemer G, Pouyssegur J (2008) Tumor cell metabolism: Cancer's Achilles' heel. *Cancer Cell* 13:472–482.
5. Vousden KH, Ryan KM (2009) p53 and metabolism. *Nat Rev Cancer* 9:691–700.
6. Schwartzenberg-Bar-Yoseph F, Armoni M, Karnieli E (2004) The tumor suppressor p53 down-regulates glucose transporters GLUT1 and GLUT4 gene expression. *Cancer Res* 64:2627–2633.
7. Bensaad K, Vousden KH (2007) p53: New roles in metabolism. *Trends Cell Biol* 17: 286–291.
8. Kondoh H, et al. (2005) Glycolytic enzymes can modulate cellular life span. *Cancer Res* 65:177–185.
9. Suzuki S, et al. (2010) Phosphate-activated glutaminase (GLS2), a p53-inducible regulator of glutamine metabolism and reactive oxygen species. *Proc Natl Acad Sci USA* 107:7461–7466.
10. Li T, et al. (2012) Tumor suppression in the absence of p53-mediated cell-cycle arrest, apoptosis, and senescence. *Cell* 149:1269–1283.
11. Kulawiec M, Ayyasamy V, Singh KK (2009) p53 regulates mtDNA copy number and mitocheckpoint pathway. *J Carcinog* 8:8.
12. Lebedeva MA, Eaton JS, Shadel GS (2009) Loss of p53 causes mitochondrial DNA depletion and altered mitochondrial reactive oxygen species homeostasis. *Biochim Biophys Acta* 1787:328–334.
13. Okamura S, et al. (1999) Identification of seven genes regulated by wild-type p53 in a colon cancer cell line carrying a well-controlled wild-type p53 expression system. *Oncol Res* 11:281–285.
14. Matoba S, et al. (2006) p53 regulates mitochondrial respiration. *Science* 312: 1650–1653.
15. Bourdon A, et al. (2007) Mutation of RRM2B, encoding p53-controlled ribonucleotide reductase (p53R2), causes severe mitochondrial DNA depletion. *Nat Genet* 39: 776–780.
16. Rolfe DF, Brown GC (1997) Cellular energy utilization and molecular origin of standard metabolic rate in mammals. *Physiol Rev* 77:731–758.
17. Herst PM, Tan AS, Scarlett DJ, Berridge MV (2004) Cell surface oxygen consumption by mitochondrial gene knockout cells. *Biochim Biophys Acta* 1656:79–87.
18. Pedersen PL (2007) Warburg, me and Hexokinase 2: Multiple discoveries of key molecular events underlying one of cancers' most common phenotypes, the "Warburg effect", i.e., elevated glycolysis in the presence of oxygen. *J Bioenerg Biomembr* 39: 211–222.
19. Wu M, et al. (2007) Multiparameter metabolic analysis reveals a close link between attenuated mitochondrial bioenergetic function and enhanced glycolysis dependency in human tumor cells. *Am J Physiol Cell Physiol* 292:C125–C136.
20. Gong Y, Dou LJ, Liang J (2014) Link between obesity and cancer: Role of triglyceride/ free fatty acid cycling. *Eur Rev Med Pharmacol Sci* 18:2808–2820.
21. Wallace DC (2012) Mitochondria and cancer. *Nat Rev Cancer* 12:685–698.
22. Schägger H, Pfeiffer K (2000) Supercomplexes in the respiratory chains of yeast and mammalian mitochondria. *EMBO J* 19:1777–1783.
23. Ikeda K, Shiba S, Horie-Inoue K, Shimokata K, Inoue S (2013) A stabilizing factor for mitochondrial respiratory supercomplex assembly regulates energy metabolism in muscle. *Nat Commun* 4:2147.
24. Rhodes DR, et al. (2007) Oncomine 3.0: Genes, pathways, and networks in a collection of 18,000 cancer gene expression profiles. *Neoplasia* 9:166–180.
25. Gyorffy B, Lánczky A, Szállási Z (2012) Implementing an online tool for genome-wide validation of survival-associated biomarkers in ovarian-cancer using microarray data from 1287 patients. *Endocr Relat Cancer* 19:197–208.
26. Györffy B, et al. (2010) An online survival analysis tool to rapidly assess the effect of 22,277 genes on breast cancer prognosis using microarray data of 1,809 patients. *Breast Cancer Res Treat* 123:725–731.
27. Wang LH, Strittmatter SM (1997) Brain CRMP forms heterotetramers similar to liver dihydropyrimidinase. *J Neurochem* 69:2261–2269.
28. Goshima Y, Nakamura F, Strittmatter P, Strittmatter SM (1995) Collapsin-induced growth cone collapse mediated by an intracellular protein related to UNC-33. *Nature* 376:509–514.
29. Wang LH, Strittmatter SM (1996) A family of rat CRMP genes is differentially expressed in the nervous system. *J Neurosci* 16:6197–6207.
30. Shih JY, et al. (2001) Collapsin response mediator protein-1 and the invasion and metastasis of cancer cells. *J Natl Cancer Inst* 93:1392–1400.
31. Pan SH, et al. (2011) The ability of LCRMP-1 to promote cancer invasion by enhancing filopodia formation is antagonized by CRMP-1. *J Clin Invest* 121:3189–3205.
32. Meyronet D, et al. (2008) Extensive expression of collapsin response mediator protein 5 (CRMP5) is a specific marker of high-grade lung neuroendocrine carcinoma. *Am J Surg Pathol* 32:1699–1708.
33. Lapuente-Brun E, et al. (2013) Supercomplex assembly determines electron flux in the mitochondrial electron transport chain. *Science* 340:1567–1570.
34. Cogliati S, et al. (2016) Mechanism of super-assembly of respiratory complexes III and IV. *Nature* 539:579–582.
35. Shiba S, et al. (2017) Deficiency of COX7RP, a mitochondrial supercomplex assembly promoting factor, lowers blood glucose level in mice. *Sci Rep* 7:7606.
36. Milenkovic D, Blaza JN, Larsson NG, Hirst J (2017) The enigma of the respiratory chain supercomplex. *Cell Metab* 25:765–776.
37. Sablina AA, et al. (2005) The antioxidant function of the p53 tumor suppressor. *Nat Med* 11:1306–1313.
38. Ni Y, et al. (2012) Germline SDHx variants modify breast and thyroid cancer risks in Cowden and Cowden-like syndrome via FAD/NAD-dependant destabilization of p53. *Hum Mol Genet* 21:300–310.
39. Minamino T, et al. (2009) A crucial role for adipose tissue p53 in the regulation of insulin resistance. *Nat Med* 15:1082–1087.
40. Lau D, Bading H (2009) Synaptic activity-mediated suppression of p53 and induction of nuclear calcium-regulated neuroprotective genes promote survival through inhibition of mitochondrial permeability transition. *J Neurosci* 29:4420–4429.
41. Lim SK, Choi YW, Lim IK, Park TJ (2012) BTG2 suppresses cancer cell migration through inhibition of Src-FAK signaling by downregulation of reactive oxygen species generation in mitochondria. *Clin Exp Metastasis* 29:901–913.
42. Scorziello A, et al. (2013) NCX3 regulates mitochondrial Ca(2+) handling through the AKAP121-anchored signaling complex and prevents hypoxia-induced neuronal death. *J Cell Sci* 126:5566–5577.

CELL BIOLOGY